One-dimensional commensurate-incommensurate transition: Bromide on the Au(100) electrode

B. M. Ocko and O. M. Magnussen
Department of Physics, Brookhaven National Laboratory, Upton, New York 11973

J. X. Wang
Department of Applied Science, Brookhaven National Laboratory, Upton, New York 11973

Th. Wandlowski
Department of Electrochemistry, University of Ulm, D-89069 Ulm, Germany

(Received 13 December 1995)

In an electrochemical environment, bromide adsorbed on the Au(100) surface forms a commensurate $c(\sqrt{2}\times 2\sqrt{2})R45°$ monolayer over a range of applied potentials. At a critical potential the bromide monolayer undergoes a transition to a uniaxial-incommensurate $c(\sqrt{2}\times p)R45°$ monolayer, where p continuously decreases from $2\sqrt{2}$ with increasing potential. In the incommensurate phase, the data support an atomic model with uniform compression rather than sharp, well-ordered domain walls. The quadratic scaling of the peak widths with the incommensurate component of the wave vector suggests that the incommensurate phase exhibits "cumulative disorder."

For adsorbed monolayers, the commensurate (C) to uniaxial-incommensurate (UIC) transition corresponds to the loss of registry in one dimension between the monolayer and the substrate. The UIC phases have been described by Frenkel and Kontorowa[1] and Frank and Van der Merwe[2] using a one-dimensional (1D) model incorporating harmonically bound atoms in a sinusoidal corrugation potential. The lowest energy solution gives rise to commensurate regions separated by domain walls (solitons). Pokrofsky and Talapov[3] have predicted that the incommensurate phase forms from the commensurate phase when entropically wandering, noninteracting domain walls appear. They find that the incommensurabilty is proportional to both the reduced temperature and chemical potential with the same power-law exponent, $\beta=1/2$. Measurements of the commensurate-incommensurate (C-IC) transition for physisorbed atoms and molecules on graphite,[4] Xe on Pt(111),[5] and bromine intercalated graphite[6] are consistent with the predicted exponent. Despite the fundamental nature of the C-IC transition, adsorbate studies have been limited to about a half dozen systems on hexagonal faces and a complete picture has yet to emerge.

Under electrochemical conditions, the chemical potential of adsorbates can be directly controlled through the applied electrode potential. The atomic level structure and phase behavior of the ensuing monolayer phases can be determined under *in situ* electrochemical conditions using both surface x-ray scattering (SXS) and scanning tunneling microscopy (STM) techniques. Previous investigations, for electrodeposited metal and halide monolayers on a variety of low-index crystal faces of Au, Ag, and Pt, have revealed many different types of commensurate and incommensurate structures and the subsequent structural phase transitions are always first order. A characteristic aspect of these incommensurate structures is that they always continuously compress with changing potential. None of these previous electrochemical studies revealed a continuous C-IC transition. Here we report the finding that the bromide monolayer on the Au(100) electrode—an underlying square substrate—does indeed undergo a C-IC transition where a commensurate $c(\sqrt{2}\times 2\sqrt{2})R45°$ structure continuously transforms to an incommensurate $c(\sqrt{2}\times p)R45°$ structure ($p\leqslant 2\sqrt{2}$).

The phase behavior of adsorbates on electrode surfaces is delineated by peaks in the cyclic voltametry (CV). For Au(100) in 0.05-M NaBr (see Fig. 1), three sharp peaks ($P1$, $P2$, $P3$) are observed in the positive sweep between -0.25 and 0.60 V referenced to the saturated calomel electrode (SCE). A detailed account of the electrochemical measurements will be published elsewhere.[7] Peak $P1$ corresponds to the rearrangement of the top gold layers from hexagonal (reconstructed) to an ideally terminated (1×1) surface.[8] The comparison of the CV (left abscissa) with the

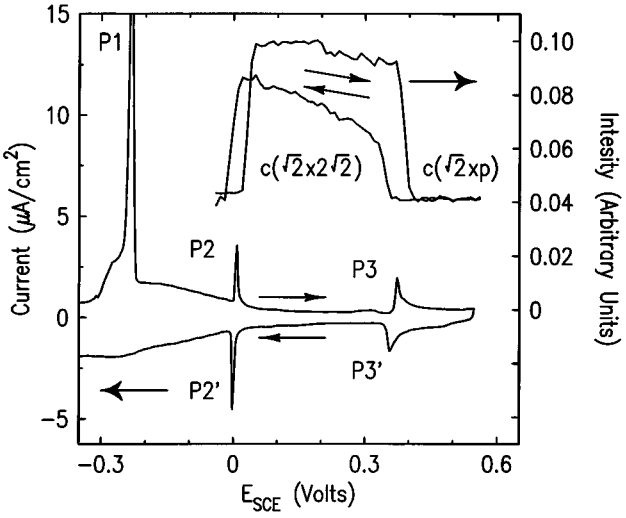

FIG. 1. Cyclic voltammogram (10 mV/sec) and the corresponding (0,1) x-ray intensity vs potential curve (1 mV/sec) from the Au(100) electrode in 0.05-M NaBr.

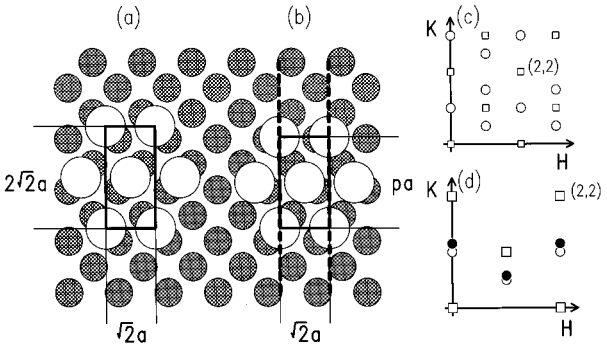

FIG. 2. Real-space sketch (a,b) of the commensurate $c(\sqrt{2}\times 2\sqrt{2})R45°$ and incommensurate $c(\sqrt{2}\times p)R45°$ phase (Br atoms are shaded circles) and the corresponding reciprocal-space patterns (c,d). In (c,d) the squares correspond to the substrate, and the circles to Br reflections. In the incommensurate phase (d), the commensurate peaks (filled circles) move outward along K with increasing potential.

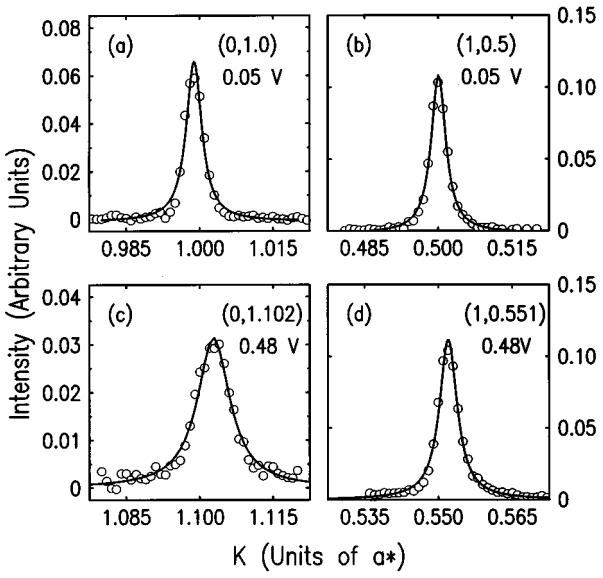

FIG. 3. X-ray scattering profiles (circles) in the commensurate phase (a,b) and incommensurate phase (c,d) through the two lowest-order peaks in reciprocal space. In (c,d), $\epsilon=0.102$ at 0.48 V. The solid lines are Lorentzian fits where the HWHM are 0.0018, 0.0018, 0.0023, and $0.0040a^*$ for (a–d), respectively.

potential dependent x-ray scattering intensity at the (0,1) position (right abscissa) indicates that the potential region between $P2/P2'$ and $P3/P3'$ corresponds to the commensurate $c(\sqrt{2}\times 2\sqrt{2})R45°$ bromide monolayer phase (discussed below) with a coverage $\theta=1/2$. This structure has also been identified for I and Cl on Au(100).[9,10] The asymmetric and slightly irreversible peaks $P3/P3'$ correspond to the C-IC transition. With both techniques the transition $P3/P3'$ exhibits rather similar hysteresis. From the potential shift in the x-ray and electrochemical features with concentration, we ascertain that the adsorbed Br is nearly fully charged.[7]

The x-ray diffraction measurements were carried out at beamlines X22 (A and B) at the National Synchrotron Light Source in the grazing incident angle geometry. Several different resolution configurations were utilized with λ ranging between 1.20 and 1.77 Å. The best radial in-plane resolution, ≈ 0.0018 Å^{-1} half width at half maximum (HWHM), was obtained at X22A using a LiF(200) analyzer crystal.[11] Typically, the gold mosaic, 0.08° HWHM, limits the transverse resolution. The reciprocal-space wave vector (H,K,L) corresponds to the standard fcc coordinates ($a=b=c=4.078$ Å with four atoms per unit cell, and $a^*=b^*=c^*=2\pi/a$), where L is along the surface normal direction. In the following, we refer to (H,K,L) as (H,K) since all measurements were carried out with $L=0.1$. As expected for the gold fcc lattice, diffraction spots are observed at the integer (H,K) positions when $H+K$ is even.

The increased diffracted intensity at (0,1) between $P2$ and $P3$ (shown in Fig. 1) signifies the existence of an ordered bromide layer. Diffraction at this position is expected for the commonly observed $c(2\times 2)$ structure ($\theta=1/2$) where the adatoms reside in the high-symmetry fourfold hollow sites. The $c(2\times 2)$ assignment, however, cannot be rationalized on the basis of the equally intense scattering observed at (0.5,1) which is forbidden for the $c(2\times 2)$ phase. Rather, the scattering is consistent with the $c(\sqrt{2}\times 2\sqrt{2})R45°$ arrangement shown in Fig. 2(a), also with $\theta=1/2$. A similar Br structure has been observed for vapor-deposited Br on Au(100).[12] That the $c(\sqrt{2}\times 2\sqrt{2})R45°$ structure is much closer to a hexagonal arrangement than the square $c(2\times 2)$ phase supports the notion that the bromide atoms would prefer to pack hexagonally in the absence of the substrate. To prove that the structure is indeed $c(\sqrt{2}\times 2\sqrt{2})R45°$, we have mapped out the diffraction (positions and intensities) at 0.05 V. There are two orthogonal directions which the $c(\sqrt{2}\times 2\sqrt{2})R45°$ phase can form on the square Au(100) substrate. Most of the observed reflections (eight out of the ten symmetry equivalents) are attributed to an undistorted commensurate Br adlayer with the centered-rectangular unit cell $c(\sqrt{2}\times 2\sqrt{2})R45°$, shown as circles in Fig. 2(a). Observed reflections at (2,1/2) and (2,3/2), which are not expected on the basis of structure factor calculations, appear to be artifacts of substrate distortions.

Whereas the adlayer symmetry is given by the diffraction pattern, the registry is not. On the basis of additional information (see below), we assert that the adatoms occupy bridge positions. For this adsorption site—based on structure factor calculations—the intensity at (1,1,0) should be coverage independent. Alternatively, the fourfold assignment gives a noticeable decrease. At (1,1,0.1), the intensity is virtually potential independent, consistent with the bridge site assignment. Second, this is also supported by STM studies for I on Au(100) which forms the same $c(\sqrt{2}\times 2\sqrt{2})R45°$ phase.[9] Since the STM images do not show periodic height modulations, all of the iodide appear to occupy the same bridge sites rather than mixed sites.

Diffraction profiles along with Lorentzian fits (solid lines) in the commensurate phase (0.05 V) are shown in Figs. 3(a,b). At 0.05 V (after cycling from -0.05 V), the K widths at (0,1) and (1,1/2) are both $0.0018a^*$ HWHM, which is only 10% broader than the spectrometer resolution.[11] However, within the same phase at 0.36 V (after cycling from 0.50 V) peaks as broad as $0.0050a^*$ are observed. The integrated intensity does not depend on the potential history. This indi-

cates that the nucleation and growth of the commensurate phase from the fluid phase yields a surface which is much better ordered than when it is formed from the incommensurate phase.

At potentials positive of $P3$ (0.38 V), the bromide adlayer undergoes a C-IC transition where the low-order diffraction features move continuously and uniaxially outward with increasing potential. As indicated by Fig. 2(d), reflections are only observed at $(1,0.5+\epsilon/2)$, $(0,1+\epsilon)$, and $(2,1+\epsilon)$, along with symmetry equivalents. In comparison, ten distinct peaks are observed in the commensurate phase. The real-space model of the UIC phase is shown in Fig. 2(b). For the domain shown, the bromide lattice is commensurate along H (the $\sqrt{2}$ direction) and incommensurate along K. As the lattice compresses the bromide atoms slide along the ''rails'' [shown as the dashed lines in Fig. 2(b)] defined by the underlying gold atoms. Most likely, the adatoms are not perfectly aligned with these rails but are locally distorted such that their proximity to the top sites is decreased.[12]

Disorder in the incommensurate phase is reflected in the shape of the diffracted profiles. In Figs. 3(c,d) we show K scans through the peaks at (0,1.102) and (1,0.551), where the Lorentzian widths are $0.0040a^*$ and $0.0023a^*$, respectively. In order to account for the intrinsic spectrometer and sample resolutions, we assume that the resolution width is equal to its commensurate value ($0.0018a^*$) and the excess width is obtained by subtraction. At 0.48 V, for instance, the excess longitudinal widths are $0.0022a^*$ and $0.0005a^*$. Surprisingly, these two widths differ by about a factor of 4. As the C-IC transition is approached from the IC side the excess widths increase continuously by an order of magnitude and far exceed the resolution limit. At $(0,1+\epsilon)$ we find that the excess longitudinal width scales inversely with ϵ as 2.5×10^{-5} Å$^{-1}/\epsilon$ and at $(0.5,0.5+\epsilon/2)$ the corresponding excess widths are three to five times smaller. For these two reciprocal-space positions, which differ by a factor of 2 in their incommensurate wave-vector components, the excess widths scale quadratically with this wave-vector component. This scaling relationship is consistent with the notion of ''cumulative disorder.'' Here the positional uncertainty, $u(R)$, between two atoms is proportional to the $\sqrt{R}$, where R is the separation between the two atoms[13] projected along the incommensurate direction. It is important to point out that this square-root relationship increases much more rapidly than the logarithmic divergence calculated for harmonically bound atoms in two dimensions. A similar square-root scaling of the Lorentzian diffraction widths has been observed for Hg chains in $Hg_{3-\delta}AsF_6$.[14] This result has been derived rigorously for the 1D harmonic Hamiltonian,[13] where the q-dependent Lorentzian widths are calculated from the measured sound velocity. For Br on Au(100), the observed quadratic scaling may result from random pinning effects which can also give rise to the quadratic form. This pinning model is also consistent with the hysteresis in the incommensurability shown in Fig. 4.

In Fig. 4(b) we show ϵ versus the applied potential in both sweep directions. A significant hysteresis is observed despite the slow effective sweep rates which range between 0.01 and 0.04 mV/sec. Additional cycles (not shown) are nearly indistinguishable. Repetitive measurements over a 30-min period showed less than a 0.1% shift in ϵ, suggesting

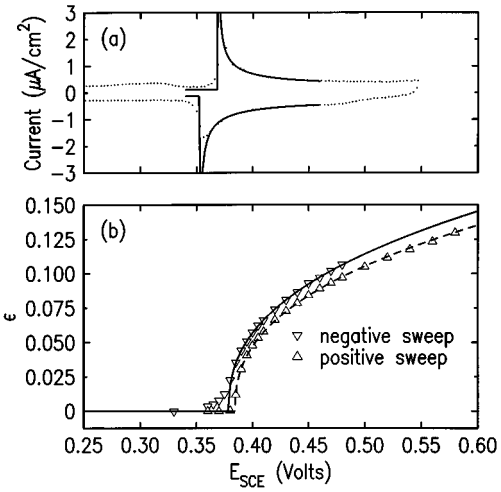

FIG. 4. (a) Cyclic voltammogram [enlarged from 1(a)]. (b) Corresponding incommensurability (ϵ) as a function of the applied potential. The solid line is a power-law fit to the incommensurabilty with $\beta=0.40$.

that the hysteresis shown in Fig. 4(b) is intrinsic. The hysteresis observed in the CV shown in Fig. 4(a) (taken at a much faster sweep rate) is comparable to that exhibited in the x-ray measurements. Hysteretic effects have also been observed for the uniaxial-incommensurate phase of I on the Au(111) electrode.[15] Even greater hysteresis is typically observed in nonelectrochemical systems.[17]

The nature or absence of satellite peaks provides information on the nature of the boundary between regions which are locally commensurate (discommensurations). The intensity of these peaks is determined from structure factor calculations using a unit cell which is $(2,D)$, where $D=a/\epsilon$ is the distance between the discommensurations. In the event of sharp, well-ordered domain walls the satellite peaks are strong, whereas they are absent for uniform compression. The absence of satellite peaks, despite an exhaustive search at several potentials, is incompatible with a well-ordered arrangement of periodic discommensurations. Either the discommensurations are locally sharp but entropically wandering or they are nearly as large as D. For the former, one would expect an increase in the transverse widths as the ''domain-wall line energy'' decreases close to the transition. The absence of such an increase at small ϵ and the absence of a ''lock-in'' transition at the high-order commensurate positions seems to favor the uniform compression model.

In the UIC phase, the nearest-neighbor (NN) distance is always 4.078 Å; however, the next-nearest-neighbor (NNN) spacing decreases from 4.56 Å for $\epsilon=0$ (commensurate) to 4.14 Å when $\epsilon=0.13$. The latter is close to the minimum Br spacing, 4.02 Å, observed on Au(111).[16] The distortion from hexagonal symmetry, given as the ratio of the NNN and NN distances, decreases from 11.7% to 1.4% over the measured range. Despite this small distortion, the bromide coverage on Au(100) is 3% less than its value at the same potential on the (111) face, where the Br monolayer is always hexagonal.[16] (The positive potential limit, on both surfaces, is limited by Au oxidation.) These minimum spacings are close to the van

der Waals diameter of Br (3.7–4.0 Å) (Ref. 18) but larger than the minimum Br spacing of 3.89 Å measured on the Pt(111) electrode.[19]

We have fitted the incommensurability to the power-law form $\epsilon=\epsilon_0(E-E_c)^\beta$ where all three parameters are allowed to vary. In the positive sweep, the power-law fit, shown as the dashed line in Fig. 4(b), provides an excellent description over the entire range with $\beta=0.40\pm0.02$, $E_c=0.385$ V, and $\epsilon_0=0.265$. An equivalent fit is obtained in the other scan direction, albeit over a range restricted to $\epsilon>0.02$, with the same β, $E_c=0.379$ V, and $\epsilon_0=0.250$. The CV current [shown in Fig. 4(a) as the dotted line] in the IC phase can be approximated as $i=i_0(E-E_c)^{\beta-1}+i_1$, where the first term is proportional to the coverage derivative with respect to the potential and the second term is related to the double layer capacitance, assumed to be constant. Fits to this form, shown as solid lines in Fig. 4(a), where $\beta=0.4$ and the other parameters are allowed to vary, describe the initial divergent-like increase as the transition is approached, but fail to describe the more rounded appearance of the data close to the *C*-IC transition. Thus, the asymmetric CV features of the *C*-IC transition (rarely observed) can be well explained by the x-ray data.

The measured exponent $\beta=0.4$ is smaller than the theoretical exponent of 1/2.[3] The theoretical prediction is only supposed to apply close to the transition, where the domain walls are narrow relative to their separation. Thus, the prediction might only apply close to the transition, where it is difficult to quantitatively extract the exponent. For Xe on Pt(111),[5] the data are only consistent with theory for $\epsilon<0.04$. On Au(100) at potentials above 0.45 V, the slope of the Br coverage with respect to potential is similar to that on Au(111).[16] Thus, the coverage at the high ϵ is not controlled by the proximity to the *C*-IC transition, but rather the two-dimensional compressibility, independent of the underlying lattice symmetry.

Our results for bromide monolayers on Au(100), under electrochemical control, indicate that the continuous commensurate to uniaxial-incommensurate transition is not restricted to the vacuum environment. The potential dependent structure of the bromide monolayer is in excellent agreement with the features observed in the electrochemical measurements. From the x-ray results, we find no evidence for sharp domain walls in the uniaxial-incommensurate phase; rather the atoms are more appropriately described by a uniform compression. This indicates that the substrate potential is weakly modulated and that the adatom-adatom interactions play a dominant role in determining the phase behavior. These results are relevant to developing a fundamental understanding of the microscopic basis of potential-induced compression in electrochemistry and to understanding the nature of the commensurate-incommensurate transition in physics. Future studies, on other electrodes, will aid in this endeavor.

This work was supported by DOE, under Contract No. DE-AC02-76CH00016. T.W. would like to thank the Deutsche Forschungsgemeinshaft. B.O. would like to thank the Weizmann Institute of Science for their support during the preparation of this manuscript.

[1] Y.I. Frenkel and T. Kontorowa, Zh. Éksp. Teor. Fiz. **8**, 1340 (1938).
[2] F.C. Frank and J.H. Van der Merwe, Proc. R. Soc. London **198**, 205 (1949).
[3] V.L. Pokrofsky and A.L. Talapov, Phys. Rev. Lett. **42**, 66 (1979).
[4] See, for instance, K.L. D'Amico *et al.*, Phys. Rev. B **41**, 4368 (1990).
[5] K. Kern and G. Cosma, in *Chemistry and Physics of Solids VII*, edited by R. Vanselow and R.F. Howe (Springer-Verlag, Berlin, 1988), p. 65.
[6] S.G.J. Mochrie, A.R. Kortan, R.J. Birgeneau, and P.M. Horn, Z. Phys. **62**, 79 (1985).
[7] Th. Wandlowski, J.X. Wang, O.M. Magnussen, and B.M. Ocko (unpublished).
[8] B.M. Ocko, J. Wang, A. Davenport, and H. Isaacs, Phys. Rev. Lett. **65**, 1466 (1990).
[9] X. Gao, G.J. Edens, F.C. Liu, A. Hamelin, and M.J. Weaver, J. Phys. Chem. **98**, 8086 (1994).
[10] B.M. Ocko, O.M. Magnussen, J.X. Wang, and Th. Wandlowski, Physica B (to be published).
[11] At X22A the radial diffraction width of $0.0016a^*$ obtained at (1,1) is slightly broader than the direct beamwidth of $0.0012a^*$.
[12] E. Bertel and F.P. Netzer, Surf. Sci. **97**, 409 (1980).
[13] V.J. Emery and J.D. Axe, Phys. Rev. Lett. **40**, 1507 (1978).
[14] J.M. Hastings *et al.*, Phys. Rev. Lett. **39**, 1484 (1977).
[15] B.M. Ocko, G.M. Watson, and J. Wang, J. Phys. Chem. **98**, 897 (1994).
[16] O.M. Magnussen, B.M. Ocko, J.X. Wang, and R.R. Adžić, Phys. Rev. B **51**, 5510 (1995).
[17] See, for instance, R.M. Fleming, D.E. Moncton, J.D. Axe, and G.S. Brown, Phys. Rev. B **30**, 1877 (1995).
[18] A.J. Bondi, J. Phys. Chem. **68**, 441 (1964).
[19] C. A. Lucas, N.M. Marković, and P.N. Ross, Surf. Sci. Lett. **340**, L949 (1995).